

## Terahertz-frequency photoconductive detectors fabricated from metal-organic chemical vapor deposition-grown Fe-doped InGaAs

O. Hatem, J. Cunningham, E. H. Linfield, C. D. Wood, A. G. Davies et al.

Citation: [Appl. Phys. Lett.](#) **98**, 121107 (2011); doi: 10.1063/1.3571289

View online: <http://dx.doi.org/10.1063/1.3571289>

View Table of Contents: <http://apl.aip.org/resource/1/APPLAB/v98/i12>

Published by the [American Institute of Physics](#).

---

### Related Articles

High-performance photodetectors for visible and near-infrared lights based on individual WS<sub>2</sub> nanotubes  
[Appl. Phys. Lett.](#) **100**, 243101 (2012)

Graphene/ZnO nanowire/graphene vertical structure based fast-response ultraviolet photodetector  
[Appl. Phys. Lett.](#) **100**, 223114 (2012)

Monolithically integrated, resonant-cavity-enhanced dual-band mid-infrared photodetector on silicon  
[Appl. Phys. Lett.](#) **100**, 211106 (2012)

Screen printed ZnO ultraviolet photoconductive sensor on pencil drawn circuitry over paper  
[Appl. Phys. Lett.](#) **100**, 211104 (2012)

ZnO nanowire based visible-transparent ultraviolet detectors on polymer substrates  
[J. Appl. Phys.](#) **111**, 102806 (2012)

---

### Additional information on [Appl. Phys. Lett.](#)

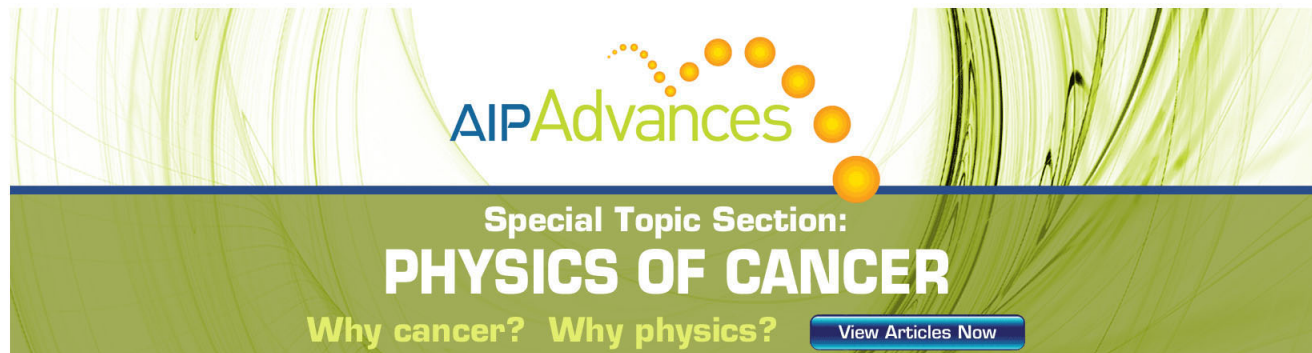
Journal Homepage: <http://apl.aip.org/>

Journal Information: [http://apl.aip.org/about/about\\_the\\_journal](http://apl.aip.org/about/about_the_journal)

Top downloads: [http://apl.aip.org/features/most\\_downloaded](http://apl.aip.org/features/most_downloaded)

Information for Authors: <http://apl.aip.org/authors>

## ADVERTISEMENT

The advertisement features a green background with abstract, flowing lines. At the top, the 'AIP Advances' logo is shown, with 'AIP' in blue and 'Advances' in green, accompanied by a series of orange dots. Below the logo, the text 'Special Topic Section: PHYSICS OF CANCER' is displayed in white, with 'PHYSICS OF CANCER' in a larger, bold font. At the bottom, the phrase 'Why cancer? Why physics?' is written in yellow, and a blue button with the text 'View Articles Now' is positioned to the right.

AIP Advances

Special Topic Section:  
**PHYSICS OF CANCER**

Why cancer? Why physics? [View Articles Now](#)

# Terahertz-frequency photoconductive detectors fabricated from metal-organic chemical vapor deposition-grown Fe-doped InGaAs

O. Hatem,<sup>1</sup> J. Cunningham,<sup>1,a)</sup> E. H. Linfield,<sup>1</sup> C. D. Wood,<sup>1</sup> A. G. Davies,<sup>1</sup> P. J. Cannard,<sup>2</sup> M. J. Robertson,<sup>2</sup> and D. G. Moodie<sup>2</sup>

<sup>1</sup>*School of Electronic and Electrical Engineering, University of Leeds, Leeds LS2 9JT, United Kingdom*

<sup>2</sup>*CIP Technologies, Adastral Park, Martlesham Heath, Ipswich, Suffolk IP5 3RE, United Kingdom*

(Received 13 January 2011; accepted 7 March 2011; published online 23 March 2011)

We report the detection of terahertz frequency radiation using photoconductive antennas fabricated from Fe-doped InGaAs, grown by metal-organic chemical vapor deposition. Coherent photoconductive detection is demonstrated using femtosecond laser pulses centered at either an 800 or a 1550 nm wavelength. The InGaAs resistivity and the sensitivity of photoconductive detection are both found to depend on the Fe-doping level. We investigate a wide range of probe laser powers, finding a peak in detected signal for  $\sim 5$  mW probe power, followed by a reduction at larger powers, attributed to screening of the detected THz field by photo-generated carriers in the material. The measured signal from Fe:InGaAs photoconductive detectors excited at 800 nm is four times greater than that from a low-temperature-grown GaAs photodetector with identical antenna design, despite the use of a ten times smaller probe power. © 2011 American Institute of Physics.

[doi:10.1063/1.3571289]

While the technique of terahertz (THz) time-domain spectroscopy (THz-TDS) (Refs. 1 and 2) has become widespread, alternative technologies to the commonly-implemented photoconductive (PC) emitters/detectors formed from low-temperature (LT)-grown GaAs are sought. Ideally, this would allow the bulky 800 nm Ti:sapphire laser systems typically used in THz-TDS systems to be replaced by more compact fiber lasers operating at 1.55  $\mu\text{m}$ , for example. Such developments are predicated on the availability of PC materials with suitably small (compared with LT-GaAs) bandgaps for photocarrier excitation. The InGaAs material system is one such candidate, with recent demonstrations in the literature showing THz emission from LT-InGaAs,<sup>3</sup> heavy-ion irradiated InGaAs,<sup>4</sup> and the emission and detection of THz radiation from Fe-implanted InGaAs.<sup>5,6</sup> In each case, the low intrinsic resistivity of InGaAs must be overcome so that a large enough surface bias field can be applied to obtain THz emission. In the case of Fe-implantation, Fe is used to reduce carrier concentration in the material to levels compatible with use of the material for PC emission. The most flexible and, we believe, most controllable method of introducing Fe-incorporation into the InGaAs lattice is through epitaxial growth. We very recently demonstrated that the technique of metal-organic chemical vapor deposition (MOCVD) provides a suitable epitaxial growth process to form high quality Fe-InGaAs that is capable of generating THz radiation through PC emission.<sup>7</sup> In this paper, we demonstrate THz PC detection using Fe-doped InGaAs, grown by MOCVD, at both 800 and 1550 nm probe wavelengths.

Table I shows the layer structure of the wafers investigated. Fe atoms were incorporated into the InGaAs during growth, to obtain a uniform concentration through the entire thickness of the Fe:InGaAs layer. The MOCVD growth conditions were identical to those recently presented in Ref. 7.

PC detectors were fabricated from three wafers (labeled 2208<sub>100</sub>, 2320<sub>0.8</sub>, and 2321<sub>0.4</sub>), grown over a wide range of Fe-doping levels ( $5 \times 10^{18} \text{ cm}^{-3}$ ,  $4 \times 10^{16} \text{ cm}^{-3}$ , and  $2 \times 10^{16} \text{ cm}^{-3}$ , respectively).

To process these wafers into PC detector devices, the top n-InP and n-InGaAs capping layers, which protected the surface of the wafer from oxidation during growth, were removed by chemical etching, and photolithography was then used to form bow-tie electrodes (with a 16  $\mu\text{m}$  gap) from evaporation of AuGeNi (300 nm thickness) on top of the Fe-InGaAs layer. A bow-tie geometry was chosen for direct comparison with existing LT-GaAs detectors already fabricated. The detectors were annealed at 300 °C for 2 min to generate Ohmic contacts between the eutectic and semiconductor. The resistivity was determined for all wafers from Hall measurements, and found to be 5  $\Omega \text{ cm}$ ,  $1 \times 10^3 \Omega \text{ cm}$ , and  $2.2 \times 10^3 \Omega \text{ cm}$ , respectively, for samples 2208<sub>100</sub>, 2320<sub>0.8</sub>, and 2321<sub>0.4</sub>. This increase in resistivity with reduction in the Fe doping concentration implies that the material was overcompensated at higher Fe doping levels.<sup>8</sup>

The apparatus used for the measurements is shown in Fig. 1, and is based on a Ti:sapphire laser (Coherent-Mira 900-P) pumped by a 14 W diode laser (Verdi V-18) operating at 532 nm. The Ti:sapphire laser produced pulses with 120 fs pulse duration at a 76 MHz repetition rate, and 830 nm wavelength. A 1.3 W average power beam from this laser was directed into a cavity-tuned optical parametric oscillator

TABLE I. Layer structure of the Fe-InGaAs wafers used in this study.

Layer	Thickness ( $\mu\text{m}$ )
n-InP (cap layer)	0.2
n-InGaAs	0.3
Fe:InGaAs	1.0
Semi-insulating InP	0.3
InP (substrate)	500

<sup>a)</sup>Author to whom correspondence should be addressed. Electronic mail: j.e.cunningham@leeds.ac.uk.

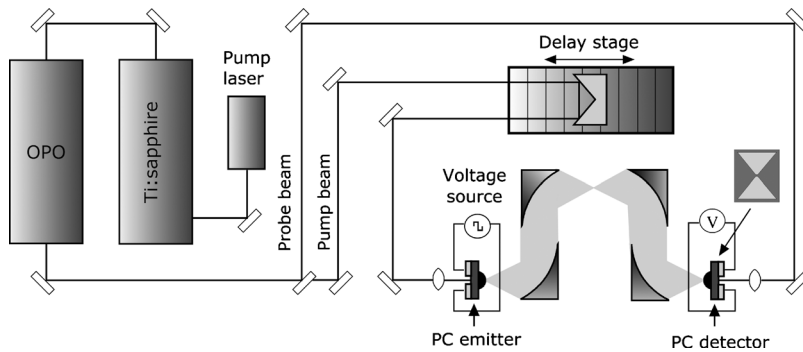


FIG. 1. THz-TDS system using a tunable OPO to generate and detect THz radiation using PC Fe-InGaAs emitters and detectors at 1550 nm.

(OPO) containing a quasiphase matched, periodically poled LiNbO<sub>3</sub> crystal. The output (tuned to 1550 nm) from the OPO was then split into two using a beam-splitter. One part (50 mW average power) was directed and focused onto a biased PC emitter (typically  $\pm 50$  V, square wave modulated at 10 kHz), with a 300  $\mu\text{m}$  electrode gap, with the laser spot positioned asymmetrically across the gap, and close to the anode, to maximize THz generation.<sup>9</sup> The emitter used for all measurements was made from wafer 2321<sub>0.4</sub>.<sup>7</sup> The other part of the OPO output (maximum power  $\sim 5$  mW), was used for coherent probing of the overlapped THz radiation at the PC detector, which measured the THz signal from the emitter, after being focused by two pairs of off-axis parabolic mirrors and hyper-hemispherical Si lenses. For comparison, measurements at an excitation wavelength of 800 nm were taken from the same emitter and detectors using a similar setup, but with a different Ti:sapphire laser (Tsunami-Spectra Physics), which generated 90 fs pulses at 800 nm. Lock-in detection of the induced voltage at the PC detector was used in both cases, based on the 10 kHz reference signal from the emitter.

Detectors made from each wafer were first tested using a 1550 nm pump and probe wavelength. Figure 2(a) shows the time-domain signals obtained from the detectors. In each case, a single-cycle pulse is clearly identified, with a full-width-half-maximum duration of  $\sim 0.6$  ps for the positive

voltage section of the half-cycle. A Fourier transform of the same data is shown in Fig. 2(b), which shows a signal-to-noise-ratio (SNR) in excess of 300:1 up to a frequency of 1.5 THz for all detectors measured. We note that this bandwidth is likely to be limited by the OPO pulse width, which was measured to be  $>200$  fs using autocorrelation. It is well known that such increased laser pulse width (relative to the more typical  $<100$  fs duration pulses obtained using an 800 nm Ti:sapphire laser) will lead to a direct reduction in the bandwidth of emitted THz signals.<sup>10</sup> The wafer with the lowest doping level (2321<sub>0.4</sub>, with a resistivity of  $2.2 \times 10^3 \Omega \text{ cm}$ ) was found to produce the highest detected signal. This may be attributed to a higher induced photocarrier concentration, resulting from the reduction in Fe trap centers throughout the wafer; we note that the detectors made from this wafer also produced the highest photocurrent of the three wafers when a dc voltage bias was introduced between the detector electrodes [Fig. 2(b) inset].

To investigate further the performance of the detectors, each was tested with (a) different biases applied to the emitter, while the pump power was maintained at a constant 50 mW on the emitter and (b) different pump powers, with a square-wave ac bias of  $\pm 60$  V applied to the emitter. A linear relationship between the THz peak amplitude and both the emitter bias voltage and the pump power was found (Fig. 3), in agreement with the standard model of PC detection.<sup>11</sup>

The detector made from the lowest doped wafer (2321<sub>0.4</sub>) was also tested at 800 nm, for comparison with a PC LT-GaAs detector formed using the same electrode spacing (16  $\mu\text{m}$ ). The same PC emitter was used in both cases, fabricated from 2321<sub>0.4</sub>, and pumped with 60 mW laser

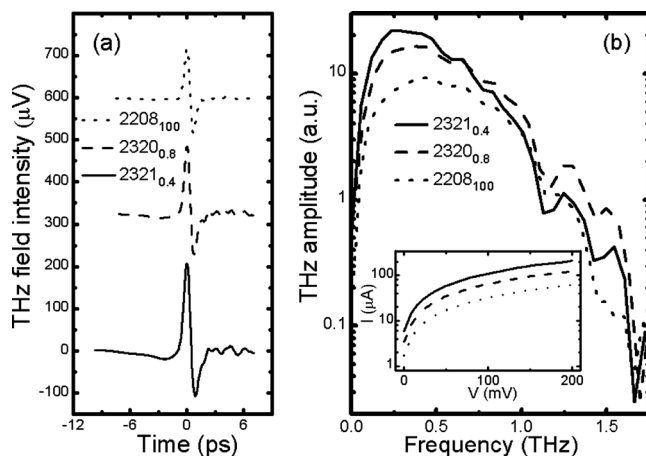


FIG. 2. (a) Time-domain and (b) frequency-domain spectra of the THz signals detected by Fe-InGaAs PC detectors excited with 5 mW probe laser power at a 1550 nm excitation wavelength, for a  $\pm 60$  V bias and 50 mW pump power applied to the emitter. In (a), the traces for wafers 2320<sub>0.8</sub> and 2208<sub>100</sub> have been vertically offset by 325  $\mu\text{V}$  and 600  $\mu\text{V}$ , respectively, for clarity. Inset to (b): the photocurrent generated from the detectors when excited with 5 mW laser at 1550 nm, as a function of applied dc bias voltage.

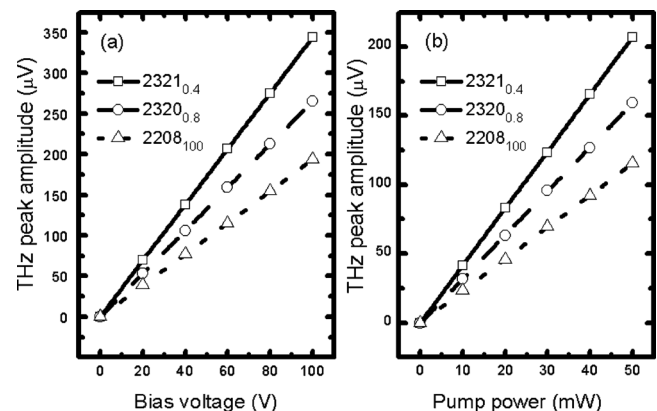


FIG. 3. THz peak amplitude from Fe-InGaAs PC detectors measured as a function of (a) the emitter bias voltage using 50 mW pump power and (b) the emitter pump power, using a  $\pm 60$  V emitter bias. In both bases the probe power was 5 mW.



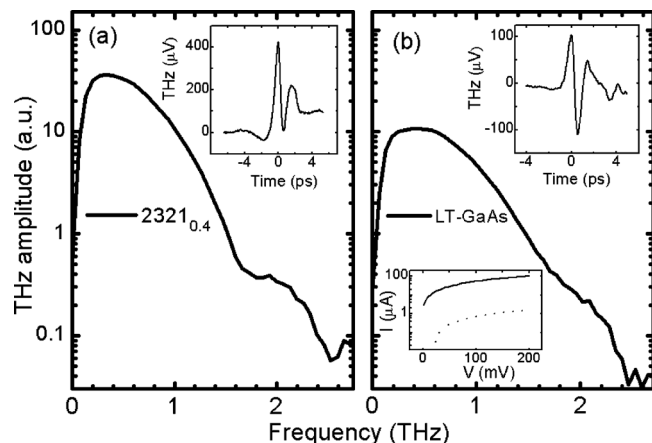


FIG. 4. (a) Frequency spectrum and (inset) the time-domain signal of the THz signal detected by an Fe-InGaAs ( $2321_{0.4}$ ) PC detector using 5 mW probe power at 800 nm. (b) Main figure: the frequency spectrum, and (upper inset) the time-domain signal of the THz signal detected by LT-GaAs PC detector using 50 mW probe power at 800 nm. Bottom inset: the photocurrent generated from the Fe-InGaAs ( $2321_{0.4}$ ) (solid) and LT-GaAs (dotted) detectors when excited with 5 mW laser power at 800 nm as a function of applied voltage.

power at 800 nm, and driven by a square-wave biased at  $\pm 100$  V. When using the Fe:InGaAs detector, 5 mW of probe power was focused onto the detector gap, while 50 mW of probe power was used for the LT-GaAs detector. Figure 4 shows the time-domain signals and frequency spectrum from both detectors. The  $2321_{0.4}$  detector showed  $\sim$ four times greater sensitivity (in terms of the amplitude of the generated voltage) than the LT-GaAs detector, but at only one-tenth of the applied probe laser power. We note also that the photocurrent was higher in the Fe:InGaAs detector (by a factor of  $>50$ ), compared with LT-GaAs (Fig. 4 inset). The bandwidth of the detected signals found from Fe:InGaAs and LT-GaAs was similar ( $\sim 2.5$  THz); this increase in bandwidth, compared with the bandwidth described above for 1550 nm excitation, reflects the shorter pulse width (90 fs) of the femto-second laser used in this case. We note that the time domain electric field response measured using the Fe-GaAs detector shows a somewhat different shape to that of the LT-GaAs detector, with more a prominent positive region, though a full three-dimensional Monte Carlo calculation of the carrier dynamics in both systems<sup>10</sup> would be required to elucidate the microscopic reasons for this discrepancy. The form of the Fourier transformed amplitude spectra is similar, despite these differences.

The  $2321_{0.4}$  detector was also tested at different probe powers, from 1 to 40 mW, using 800 nm excitation, as shown in Fig. 5. In each case, the emitter was excited with 5 mW pump power, and a square wave biased at  $\pm 60$  V. The detected THz amplitude and SNR both increased for applied probe powers up to 5 mW but then decreased as the probe power was increased further. This decrease in signal and SNR at high probe powers is likely to be caused by the increased screening of the THz electric field by the higher densities of photocarriers produced at higher probe powers. This screening appears to be more pronounced in the Fe-InGaAs than in previously investigated LT-GaAs samples<sup>12</sup> which typically show saturation rather than a decrease in signal for high power excitation.

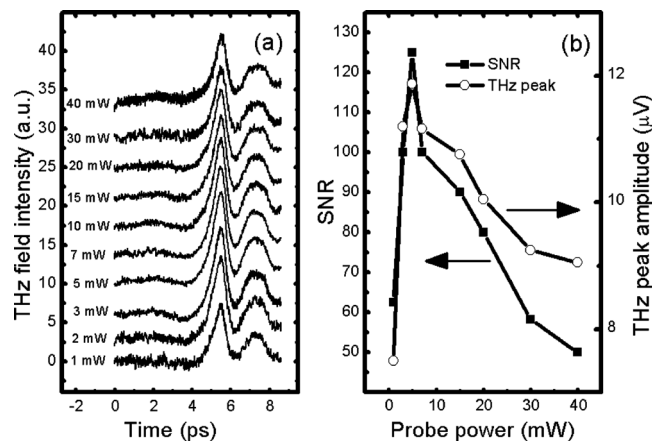


FIG. 5. (a) Time-domain signals (vertically offset by 3  $\mu\text{V}$  intervals for clarity) detected by a Fe-InGaAs ( $2321_{0.4}$ ) PC detector, at different probe powers, at 800 nm and (b) the corresponding SNR and THz peak amplitudes. The emitters were biased at  $\pm 60$  V, and pumped with 5 mW laser power.

In summary, we have demonstrated that MOCVD-grown Fe:InGaAs materials can be used as PC detectors at wavelengths of both 800 nm and  $1.55 \mu\text{m}$ . Bandwidths of 2.5 THz and 1.5 THz were obtained at 800 nm and  $1.55 \mu\text{m}$ , respectively (in both cases, limited by the laser pulse width). In each case, the Fe doping level has a significant effect on the material resistivity, and the sensitivity of detectors. We find that the measured signal from Fe:InGaAs PC detectors excited at 800 nm is four times greater than that from a LT-grown GaAs photodetector with identical antenna design, despite the use of a ten times smaller probe power. In contrast to LT-GaAs detectors, the probe power level has a substantial effect on the SNR and the detected signal amplitude. This work demonstrates the possibility of using MOCVD-grown Fe:InGaAs for compact, THz TDS systems operating at  $1.55 \mu\text{m}$ .

We acknowledge support from the EPSRC (Grant Nos. EP/D50225X, EP/H029583, and EP/F029543), and from the Egyptian government.

- <sup>1</sup>P. R. Smith, D. H. Auston, and M. C. Nuss, *IEEE J. Quantum Electron.* **24**, 255 (1988).
- <sup>2</sup>Y. C. Shen, P. C. Upadhyaya, E. H. Linfield, H. E. Beere, and A. G. Davies, *Appl. Phys. Lett.* **83**, 3117 (2003).
- <sup>3</sup>A. Takazato, M. Kamakura, T. Matsui, J. Kitagawa, and Y. Kadoya, *Appl. Phys. Lett.* **91**, 011102 (2007).
- <sup>4</sup>J. Mangeney and P. Crozat, *C. R. Phys.* **9**, 142 (2008).
- <sup>5</sup>M. Suzuki and M. Tonouchi, *Appl. Phys. Lett.* **86**, 051104 (2005).
- <sup>6</sup>M. Suzuki and M. Tonouchi, *Appl. Phys. Lett.* **86**, 163504 (2005).
- <sup>7</sup>C. D. Wood, O. Hatem, J. E. Cunningham, E. H. Linfield, A. G. Davies, P. J. Cannard, M. J. Robertson, and D. G. Moodie, *Appl. Phys. Lett.* **96**, 194104 (2010).
- <sup>8</sup>C. Rigo, M. Madella, C. Papuzza, C. Cacciatore, A. Stano, A. Gasparotto, G. Salvati, and L. Nasi, *J. Cryst. Growth* **164**, 430 (1996).
- <sup>9</sup>P. C. Upadhyaya, W. H. Fan, A. Burnett, J. Cunningham, A. G. Davies, E. H. Linfield, J. Lloyd-Hughes, E. Castro-Camus, M. B. Johnston, and H. Beere, *Opt. Lett.* **32**, 2297 (2007).
- <sup>10</sup>E. Castro-Camus, J. Lloyd-Hughes, and M. B. Johnston, *Phys. Rev. B* **71**, 195301 (2005).
- <sup>11</sup>J. T. Darrow, X. C. Zhang, and J. D. Morse, *IEEE J. Quantum Electron.* **28**, 1607 (1992).
- <sup>12</sup>C. Ludwig and J. Kuhl, *Appl. Phys. Lett.* **69**, 1194 (1996).